Available online at www.sciencedirect.com
SCIENCE DIRECT®
Biomaterials 25 (2004) 2437–2445
Biomaterials
www.elsevier.com/locate/biomaterials

Contact profilometry and correspondence analysis to correlate surface properties and cell adhesion in vitro of uncoated and coated Ti and Ti6Al4V disks

Andrea Bagno[a,*], Marco Genovese[a], Alessandra Luchini[a], Monica Dettin[a], Maria Teresa Conconi[b], Anna Michela Menti[b], Pier Paolo Parnigotto[b], Carlo Di Bello[a]

[a] Department of Chemical Process Engineering, University of Padova, via Marzolo 9, 35131 Pasova, Italy
[b] Department of Pharmaceutical Sciences, University of Padova, via Marzolo 9, 35131 Pasova, Italy

Received 12 June 2003; accepted 7 September 2003

Abstract

A fundamental goal in the field of implantology is the design of specific devices able to induce a controlled and rapid "osseointegration". This result has been achieved by means of surface modifications aimed at optimizing implant-to-bone contact; furthermore, bone cell adhesion on implant surface has been directly improved by the application of biomolecules that stimulate new tissue formation, thus controlling interactions between biological environment and implanted materials.

Actually, methods for biochemical factor delivery at the interface between implant surface and biological tissues are under investigation; a reliable technique is represented by the inclusion of biologically active molecules into biocompatible and biodegradable materials used for coating implant surface.

This paper focuses the application of three polymeric materials already acknowledged in the clinical practice, i.e. poly-L-lactic acid (PLLA), poly-DL-lactic acid (PDLA), and sodium alginate hydrogel. They have been used to coat Ti (Ti2) and Ti6Al4V (Ti5) disks; their characteristics have been determined and their performances compared, with specific regard to the ability in allowing osteoblast adhesion in vitro. Moreover, profilometry data analysis permitted to identify a specific roughness parameter (peak density) which mainly controls the amount of osteoblast adhesion.
© 2003 Elsevier Ltd. All rights reserved.

Keywords: Cell adhesion; Hydrogel; Titanium; Osteoblast; Polyglycolic acid; Polylactic acid

1. Introduction

Research and clinical experience in the field of implantology suggest that the osseointegration process is affected by different factors: anatomical location, implant size, surface and geometry, surgical procedure, loading characteristics, biological fluids, patient age and sex.

When a metallic implant is surgically placed, its surface comes in close apposition to the exposed biological tissues and this results in a sequence of different physico-chemical and biochemical events [1]; thus, the performances of implanted materials rely on the nature of the interactions between biomaterials and cells [2–4]. Basically, the specificity of cell–surface interactions depends, at least partly, on surface properties in terms of both composition and roughness [5–7]. In fact, surface characteristics directly and indirectly influence the mode of action of the different molecules present in the biological world and this might control the quality of early cell adhesion and, as a consequence, new bone tissue formation [5,8].

For all these reasons, different treatments have been performed to induce modifications in both chemical composition and topography of implant surface [9], with the aim to ameliorate bone-to-implant contacts [10,11] thus improving the osseointegration process and the biomechanical performances in the short and even in the long term [1,12].

Recent studies have identified a wide range of biochemical signals that can be exploited to promote adhesion, migration, proliferation and differentiation of

*Corresponding author. Tel.: +39-049-827-5544; fax: +39-049-827-5555.
E-mail address: andrea.bagno@unipd.it (A. Bagno).

0142-9612/$ - see front matter © 2003 Elsevier Ltd. All rights reserved.
doi:10.1016/j.biomaterials.2003.09.018

cells [6]. In fact, cell/cell and cell/surface interactions, and adhesion process as well, are mediated by cell membrane receptors, responsible for reversible, non-covalent binding to complementary ligand proteins present in the cell membrane, in the ECM, or both. These molecules can also be released on the surface of synthetic biomaterials [13].

Much research has centered on adhesive proteins (e.g., fibronectin, collagen, vitronectin, etc.) and correspondent cellular receptors. For example, the simple RGD adhesive sequence, contained in six bone-related proteins at least [14,15], has been demonstrated to play a key role in the binding to cell membrane receptors [16]; moreover, a variety of bone-related growth factors, which are produced by cells and/or stored in bone matrix, are known to mediate osteoblast functions after attachment [14]. These findings have stimulated the production of biomaterials able to elicit the desired responses from patient's body and specifically promote osteoblast actions.

Several methods have been proposed for biochemical factors delivery at the interface between implant surface and biological tissue; these include simple physico-chemical adsorption, covalent immobilization (after chemical modification of the surface, if necessary) [14,17–19], and inclusion in biocompatible and biodegradable materials used to coat implant surface [20–22].

The purpose of the present study was to investigate if and how the use of candidate coatings can affect implant surface properties and osteoblast adhesion; thus, the behavior of three different materials, whose application is already acknowledged in the clinical practice, was compared. At first, a number of Ti (Ti2) and Ti6Al4V (Ti5) disks were mechanically and chemically treated (sand-blasted and acid-attacked) to obtain homogeneously comparable substrates; afterwards, disk surface properties were characterized in terms of defect dimensions and roughness (contact profilometry).

Three polymeric materials were prepared, namely poly-L-lactic acid (PLLA), poly-DL-lactic acid (PDLA), and sodium alginate hydrogel. Thus, these materials were used to coat a part of the treated disks: surface properties of coated disks have been estimated and the capacity of uncoated and coated surfaces to allow osteoblast adhesion was compared by in vitro assays.

An explorative computational method was used to manage profilometry data, thus permitting the identification of one single roughness parameter (S_{ds}, peak density) which is mainly correlated with the amount of cell adhesion. Peak density is deemed to be responsible for the control of preliminary cell functions in contact with substrate surface. This finding might help in addressing further design of innovative coating devices able to deliver biochemical signals and promote, at the same time, bone cell adhesion.

2. Materials and methods

2.1. Titanium disks

A number of commercially pure titanium (Ti grade 2) and Ti6Al4V (Ti grade 5) disks (∅ 15 mm; height 2.5 mm) were obtained from cylindrical bars by turning. First, they were smoothed (80 or 200 Grit Paper), then sand-blasted (corundum 350 μm for 10 s), and attacked with acidic solution (7% HCl/H_2O (w/w) and 27% H_2SO_4/H_2O (w/w)) for 9 min at mixture boiling point and 60 min at room temperature for Ti and Ti6Al4V disks, respectively. Afterwards, sand-blasted, and sand-blasted and acid-attacked disks were thoroughly degreased, washed and sonicated in a sequence of solvents: ethanol (Carlo Erba, Milan, Italy), acetone (Janssen, Geel, Belgium), chloroform (LabScan, Dublin, Ireland). In the following part of the text, sand-blasted surfaces are indicated as SL; sand-blasted and acid-attacked surfaces as SLA. Ti2 identifies commercially pure titanium, while Ti5 indicates titanium alloy Ti6Al4V.

2.2. Polymeric coatings

The following polymeric materials were considered for coating SLA-Ti2 and SLA-Ti5 disks: PLLA (Sigma Chemical, Milan, Italy), PDLA (Sigma Chemical, Milan, Italy), and sodium alginate hydrogel.

In 8.75 ml of $CHCl_3$, 0.5 g of PLLA (molecular weight range: 85–160 kDa) was dissolved achieving solution final titer of 5.7 mg/ml. The solution was characterized by high vapor pressure, so it was stored at $-10^{\circ}C$.

In 0.62 ml of $CHCl_3$, 35 mg of PDLA (molecular weight range: 75–120 kDa) was dissolved achieving solution final titer of 5.8 mg/ml. The solution obtained was still characterized by high volatility, but exhibited lower viscosity and density.

Sodium alginate hydrogel was prepared as described in [22]: 0.5 g of sodium alginate (Fluka, Milan, Italy) and 50 ml demineralized water required 26.8 μl ethylendiammine (Fluka) and 0.77 g 1-ethyl-3(3-dimethyl-aminopropil)-carbodiimide hydrochloride (Sigma Aldrich, Milan, Italy), to obtain the intermediate AGA-100 gel. The gel was washed, then freeze-dried. 13 mg of AGA-100 were then added to 700 ml of demineralized water, allowing swelling.

After preparation, 70 μl of each solution were applied onto disks surfaces by mean of Gilson 200 micro-pipette and excess solvent was removed under vacuum overnight. In the case of AGA-100, water removal was improved utilizing P_2O_5 as demoisturizing agent. Polymers amounts were verified by weighing the disks before and after deposition (Mettler AE 240).

2.3. Cell culture

Osteoblasts were obtained from femurs of adult Sprague-Dowley rats according to the method proposed by Rickard et al. [23]. Cells were collected from bone marrow by repeated washings with DMEM (Dulbecco's Modified Eagle's Medium) (Sigma) supplemented with fetal bovine serum (FBS) (Seromed, Berlin, Germany) and antibiotic (Sigma). Cell suspension was centrifuged (5 min, 1500 rpm) and extracted cells were resuspended in α-MEM (α-Minimun Essential Medium) (Life Technologies, Paisley, Scotland, UK) containing 1% antibiotic-antimytotic solution (Sigma) and supplemented with the following factors: FBS 10%; glutamine (Sigma) 2 mM; ascorbic acid (Sigma) 50 μM; dexametasone (Sigma) 10^{-8} M; Ultroser (Gibco Invitrogen, San Giuliano Milanese, Italy) 2%. Five days after seeding, culture medium was replaced and added with 10 mM β-glycerophosphate (Sigma). Subconfluent cultures were removed with 0.002% EDTA (Sigma) and 0.25% trypsin (Sigma) in PBS, and centrifuged (5 min at 1500 rpm). The osteoblast phenotype was confirmed by alkaline phosphatase activity [24], formation of calcium phosphate mineral deposits (von Kossa staining [25]) and scanning electron microscopy.

2.4. Adhesion assay

Cells were removed from culture plates with 1:1 trypsin-EDTA solution; after removal, enzyme was inactivated and cells suspension was centrifuged (5 min, 1500 rpm). Cells were resuspended in their medium and counted in a Burker chamber using trypan blue (Sigma-Aldrich). Uncoated and coated SL-Ti2, SLA-Ti2, SL-Ti5 and SLA-Ti5 disks were placed into 24-well culture plates; then cells were seeded upon them (3×10^4 cell/cm^2) and allowed to adhere for 1 h. At the end of the incubation period, cultures were rinsed twofold in order to remove non-adherent cells and then fixed in 10% neutral buffered formalin. The fixed cells were stained with 0.04% cresyl violet in 20% methanol for 30 min. The dye was extracted with 0.1 M citric acid in 50% ethanol, and absorbance was determined at 570 nm with a Microplate Autoreader EL 13 (BIO-TEK Instruments, Winooski, VT). The results, means of three experiments and expressed as optical density (OD), were converted into percentage; the OD value corresponding to the cultures seeded onto uncoated SL-Ti2 disks was taken as 100%.

Due to dye retention, a different procedure was followed to determine the amount of fixed cells on AGA-100 coated disks; 1 h after seeding, the medium was removed and cultures were rinsed two-fold. Not adherent cells were determined by means of trypan blue in medium and washing solutions.

2.5. Morphological characterization

In order to characterize SL-Ti2, SL-Ti5, SLA-Ti2 and SLA-Ti5 disk surfaces, surface pictures were acquired with an optical microscope (Leica DMRM) at different magnification (from 50× up to 1000×) to focus both single defect and local defect organization. Surface defects were measured by means of image analysis software (Casti MicroImage 3.4) in terms of both width (μm) and depth (μm). These values are taken as means of 10 up to 20 measurements. A third adimensional parameter was calculated: the so-called "shape ratio", which represents how much the area of real profile increases compared with the projected one. Shape ratio allowed a rough description of the amount and relevance of surface defects.

2.6. SEM microscopy

Investigations on surface appearance, both uncoated and coated, were carried out by scanning electron microscope (Philips 525M) equipped with EDAX for chemical composition analysis, at different magnification (from 60× up to 600×).

2.7. ESEM microscopy

Cultures were fixed for 24 h with 3% glutaraldheyde in 0.1 M cacodylate buffer (pH = 7.2) and extensively washed with water. Samples were observed using Feico Philips ElectroScan FEG XL 30 ESEM field emission gun environmental scanning electron microscope, running in the so-called environmental, wet mode at 5°C and with atmosphere 4.2 bar of water vapor pressure.

2.8. Profilometer analysis

Under KLA-Tencor P10 Surface Profiler operated at 100 Hz sampling frequency and 50 μm/s scanning rate $600 \times 600\ \mu m^2$ surface areas of both uncoated and coated disks were examined. Seven roughness parameters were determined: S_a, average roughness (μm); S_q, root mean square roughness (Å); S_z, ten-points mean roughness (Å); S_{ds}, peak density (1/Å^2); S_{sk}, profile asymmetry; S_{ku}, profile kurtosis; $S_{\Delta q}$, root mean square profile slope (°).

2.9. Data analysis

Data were analyzed by means of correspondence analysis [26–28] which is an explorative computational method for the study of associations among variables. It allows to display a low-dimensional projection of the data (e.g., into a plane). It does this, though, for two variables simultaneously (biplot) [29], thus revealing associations between them. Each value of a variable is

represented by a point in the Euclidean space in such a way that the linear distance between any two points may be interpreted in terms of similarity. In addition, the angular distance between two points of different variables corresponds to the strength of the association between the corresponding categories.

3. Results and discussion

3.1. Acid attack effects on Ti and Ti6Al4V surfaces

The first experimental step was aimed at characterizing substrate materials; in particular, SL-Ti2 and SL-Ti5 surfaces original properties were determined by measuring defect width (μm), defect depth (μm) and the adimensional "shape ratio" parameter before and after acid attack (Table 1). Fig. 1 illustrates optical microscope images of sand-blasted and acid-attacked surfaces. As expected, from data and images it is possible to appreciate that acid attack produces a decrease in defect dimensions on both surfaces. It is worthwhile mentioning that, in general, SL-Ti2 is less reactive to acid attack than SL-Ti5, even though it is not possible to identify a material-dependent effect on surface defect distribution as induced by the attack: thus, acid attack conditions have to be more severe in the case of Ti2 disks.

Roughness estimation on both SL-Ti2 and SL-Ti5 surfaces, before and after acid attack, was performed: Table 2 summarizes roughness values as they have been calculated by contact profilometry and Fig. 2 illustrates the corresponding surface topography. Profilometry data indicate a deeper effect of acid attack on SL-Ti2 with respect to SL-Ti5. In particular, SL-Ti2 disks seem to lose defects of secondary dimension after acidic treatment, maintaining only the elements rising above the ground. The opposite effect is produced on SL-Ti5 disks. In order to complete the investigation on sand-blasting and acid-attack treatments, and to examine the effects of combination thereof, SEM images at different magnification of sand-blasted and acid-attacked surfaces are reported (Fig. 3). It is possible to compare

Table 1
Mean values of defect dimensions on Ti2 and Ti5 surfaces, before and after acid attack

Disk	Depth (μm)	Width (μm)	Shape ratio
SL-Ti2	20.2	118.3	2.951
SLA-Ti2	15.6	116.4	1.456
SL-Ti5	15.8	66.9	2.254
SLA-Ti2	14.3	75.6	1.381

Sand-blasted surface are indicated as SL; sand-blasted and acid-attacked surface are indicated as SLA. Ti2 identifies commercially pure titanium, while Ti5 indicates titanium alloy Ti6Al4V.

Table 2
Roughness parameters values as estimated by contact profilometry on SL-Ti2, SL-Ti5, SLA-Ti2 and SLA-Ti5 surfaces

Disk	S_a (μm)	S_q (μm)	S_z (μm)	S_{ds} (1/cm^2)	S_{sk}	S_{ku}	$S_{\Delta q}$ (°)
SL-Ti2	2.41	3.03	15.31	4.67E+05	−0.194	3.14	4.45
SLA-Ti2	4.31	5.4	26.50	4.50E+05	−0.310	3.12	6.89
SL-Ti5	3.14	3.97	22.51	4.03E+05	−0.527	3.02	5.48
SLA-Ti5	2.56	3.26	19.01	4.83E+05	−0.085	3.67	4.73

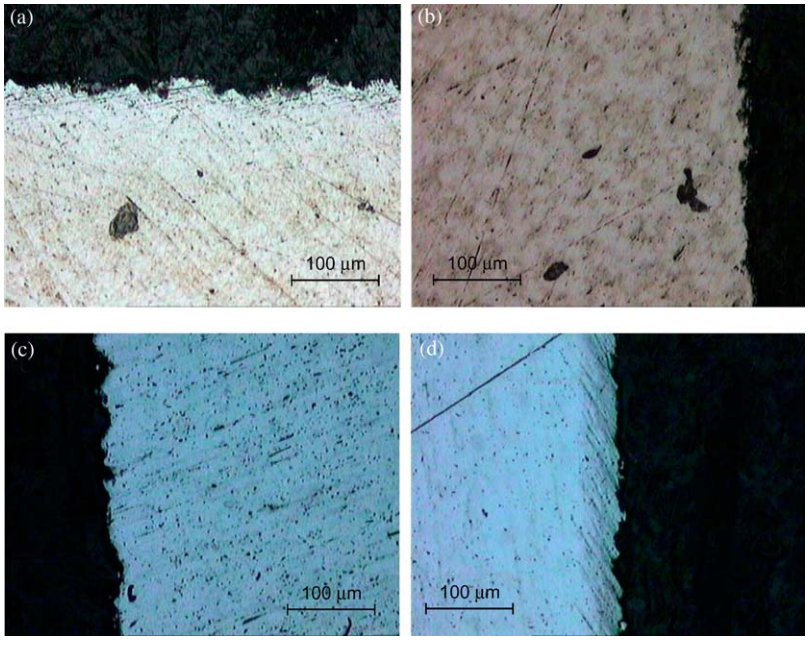

Fig. 1. Optical microscope images (100 ×) of disk surfaces: SL-Ti2 (a) and SLA-Ti2 (b); SL-Ti5 (c) and SLA-Ti5 (d).

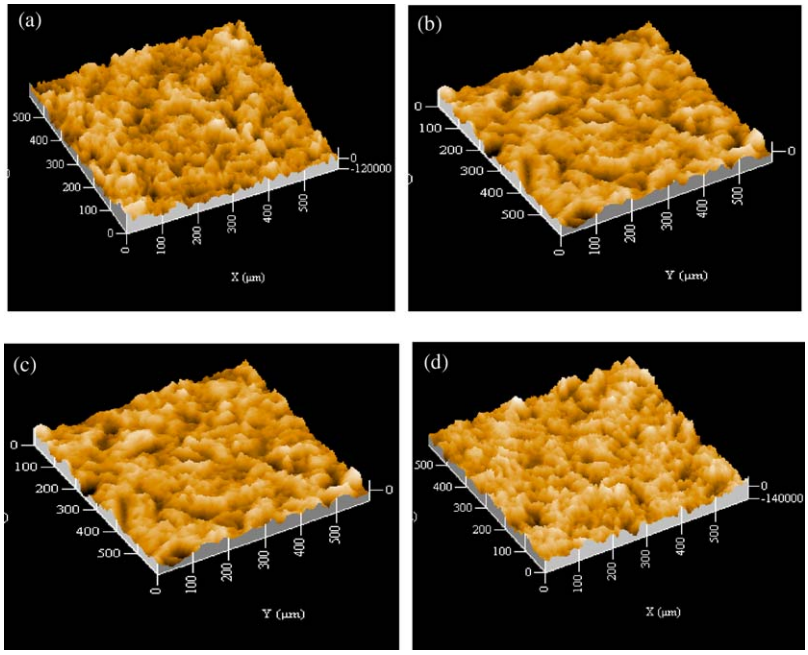

Fig. 2. Images of $600 \times 600\,\mu m^2$ areas as obtained by contact profilometry: SL-Ti2 (a) and SLA-Ti2 (b) surfaces; SL-Ti5 (c) and SLA-Ti5 (d) surfaces.

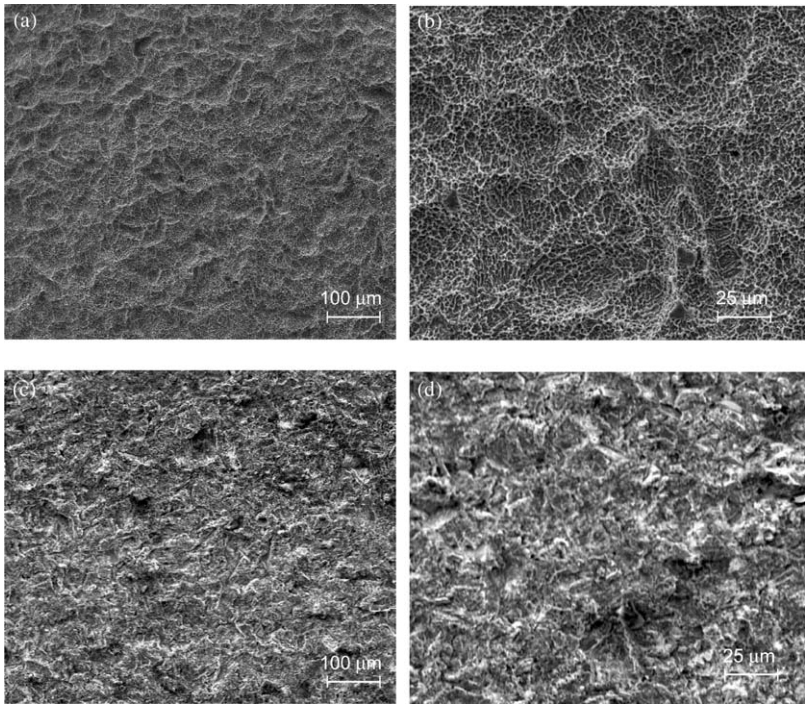

Fig. 3. SEM images of SLA-Ti2 (a, b) and SLA-Ti5 (c, d) surfaces at different magnification.

surface defects that are clearly modified on Ti2 disks more than on Ti5 ones, in terms of both dimension and distribution: the Ti2 surface exhibits a porous distribution of micro-defects among a wider topographic landscape, while the Ti5 surface reveals a more homogeneous structure.

3.2. Coated surfaces characterization

After defect dimensions characterization, SLA-Ti2 disks were coated with PLLA, PDLA, and sodium alginate hydrogel; on the other hand, SLA-Ti5 disks were coated with PLLA.

Roughness parameters were estimated for all coated surfaces (Table 3) and confirmed the indications showed by contact profilometry images (Figs. 4 and 5): the characteristics of surface topography are dramatically altered by the presence of all coating materials, but AGA-100. This latter is the only coating able to preserve, at least partially, adequate roughness properties; on the contrary, PLLA and PDLA, covering surface defects, completely mask the original roughness and make all coated surfaces smoother than the uncoated ones. In particular, Ti2 surfaces appear to be more uneven than Ti5 ones.

3.3. Adhesion assays evaluation and correspondence analysis application

Both uncoated and coated surfaces were used as substrates for in vitro osteoblast adhesion assays. Different surfaces, with different morphological properties, exhibited different behaviors with regard to the level of osteoblast adhesion.

While SLA surfaces allowed osteoblast to adhere with comparable results, coated surfaces seem to hinder osteblast from adhering, with the exception of AGA-100 coated surface (Table 4). This result can be explained on the basis of surface morphological characteristics: while PLLA and PDLA coated surfaces did not recall the original disk surface morphology, AGA-100 did. Thus, the rule of surface properties in promoting osteoblast adhesion was confirmed. A complete investigation of the effects of different coating materials has been performed on Ti2 surface only: indeed, the results obtained demonstrate that the amount of osteoblast adhesion does not depend on the nature (i.e., chemical composition) of the substrate, but on the coating used and on the topography of the surface.

An ESEM image of osteoblasts after adhesion onto AGA-100 coated SLA-Ti2 surface is reported in Fig. 6.

Roughness data and adhesion results were crossed in a tentative to identify which is/are roughness parameter/s mainly responsible for inducing/not hindering osteoblast adhesion; in other words, roughness parameters

Table 3
Roughness parameters average values as estimated by contact profilometry on SLA-Ti2 and SLA-Ti5 surfaces after coatings deposition

Disk sample	S_a (μm)	S_q (μm)	S_z (μm)	S_{ds} (1/cm^2)	S_{sk}	S_{ku}	$S_{\Delta q}$ (°)
SLA-Ti2 + PLLA	2.39	3.04	13.99	8.43E + 04	−0.107	3.24	1.79
SLA-Ti2 + PDLA	1.72	2.22	10.5	6.47E + 04	−0.299	4.23	1.58
SLA-Ti2 + AGA-100	2.78	3.51	20.92	3.77E + 05	−0.017	3.41	3.67
SLA-Ti5 + PLLA	1.37	1.77	9.95	9.37E + 04	0.007	3.87	1.36

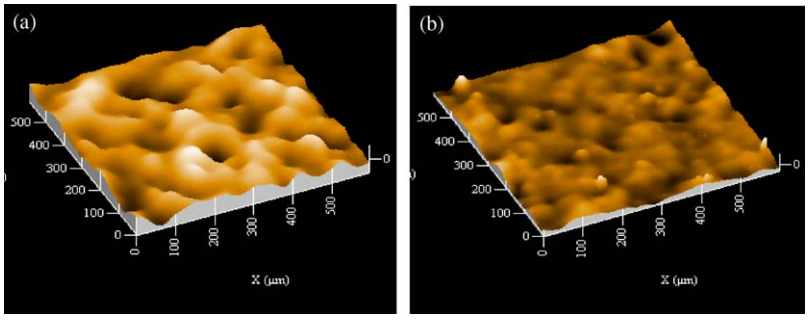

Fig. 4. Images of $600 \times 600\,\mu m^2$ areas as obtained by contact profilometry: SLA-Ti2 (a) and SLA-Ti5 (b) surfaces coated with PLLA.

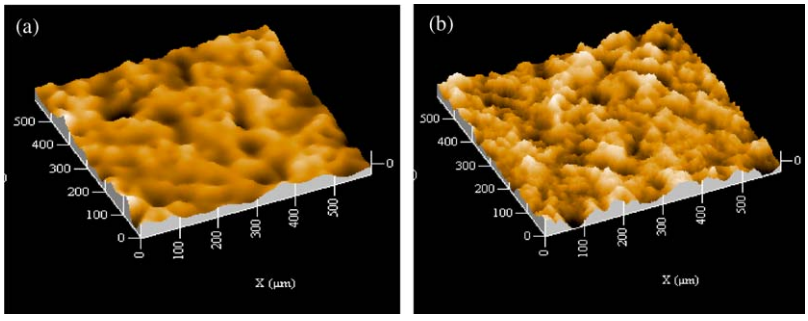

Fig. 5. Images of $600 \times 600\,\mu m^2$ areas as obtained by contact profilometry: SLA-Ti2 coated with PDLA (a) and AGA-100 (b).

Table 4
Amount of RBM osteoblast adhesion (percentage expressed as optical density, OD) as determined in vitro

Disk	OD (%)
SL-Ti2	100
SLA-Ti2	93
SLA-Ti2 + PLLA	23
SLA-Ti2 + PDLA	31
SLA-Ti2 + AGA-100	102
SL-Ti5	96
SLA-Ti5	127
SLA-Ti5 + PLLA	18

The OD value corresponding to the cultures seeded onto sand-blasted Ti disk is taken as 100%.

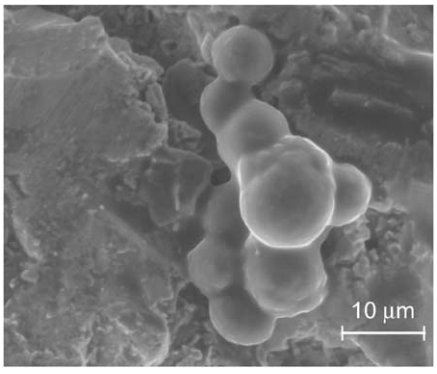

Fig. 6. ESEM image of RBM osteoblasts after adhesion on SLA-Ti2 disk coated with AGA-100: cells show high density and good organization, even though they are not yet flattened.

were correlated with adhesion results by means of correspondence analysis. This explorative computational method was applied to a numerical matrix containing positive values, which were previously normalized (Table 5). Thus, each variable was forced to assume average value 1 and to be >0. Fig. 7 illustrates a typical correspondence analysis graphical output: from the plot, it is possible to assert that S_{ds} parameter and OD values are closely correlated, based on their proximity. S_{sk} and S_{ku} parameters show a similar trend, but they are not correlated with OD values since they lie symmetrical with respect to the origin of the plane. S_a, S_q and S_z are identified by restricted, almost overlapped projections: this evidence suggests a good isotropy degree of the sampled surface areas. Finally, $S_{\Delta q}$ projection indicates a quite good correlation with OD values, as reported in literature, even though the $S_{\Delta q}$ correlation is largely overcome by S_{ds} parameter.

Moreover, from the plot it is possible to highlight the relationships among roughness and adhesion data and surface characteristics: as a matter of fact, SLA, as well as AGA-100 coated surfaces, lye in the proximity of OD representations; this means that all these surfaces share

Table 5
Sample identification as reported in the correspondence analysis graphs: three samples have been considered for each surface

Disk	Sample lables
SL-Ti2	TL1, TL2, TL3
SLA-Ti2	TLA1, TLA2, TLA3
SLA-Ti2 + PLLA	TLAL1, TLAL2, TLAL3
SLA-Ti2 + PDLA	TDL1, TDL2, TDL3
SLA-Ti2 + AGA-100	TAlg1, TAlg2, TAlg3
SL-Ti5	AL1, AL2, AL3
SLA-Ti5	ALA1, ALA2, ALA3
SLA-Ti5 + PLLA	ALAL1, ALAL2, ALAL3

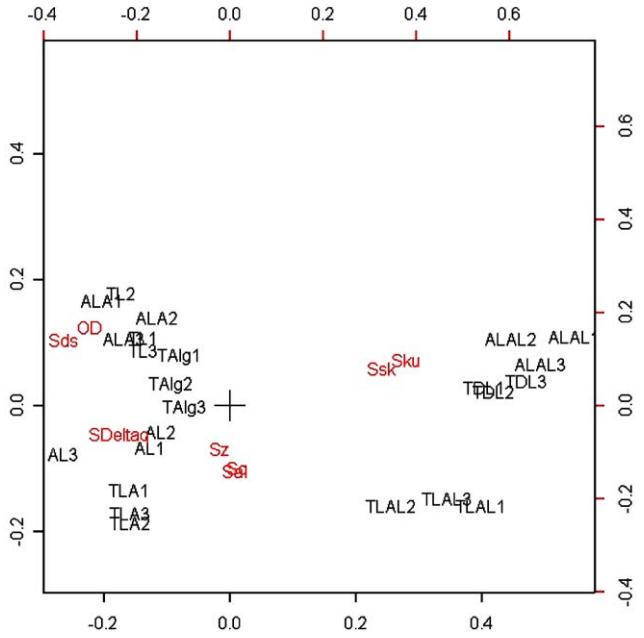

Fig. 7. Correspondence analysis results: graphical representation of roughness parameters correlated with osteoblast adhesion assay results (expressed as OD) on different surface samples.

the same favorable properties with respect to cell adhesion. At the same time, they are all characterized by high S_{ds} and, to less extent, high $S_{\Delta q}$ values. The other surface samples are located in the opposite side of the plane since they poorly perform in osteoblast adhesion process. Therefore, the most relevant information kept in the dataset is the clear discrimination among surfaces which favor or hinder cell adhesion, as quantified by OD values strictly correlated to S_{ds} and $S_{\Delta q}$ parameters.

4. Conclusions

At present, several biochemical signals are known to promote adhesion, migration, proliferation and differentiation of bone cells providing for osseointegration

and improving implant biomechanical functionality. Moreover, several materials are suitable for coating implant surface, allowing biochemical factors to be transferred and delivered at the interface between biomaterial and biological tissues.

In the present study different behaviors of three candidate coating materials have been compared: PLLA, PDLA, and AGA-100. In particular, surface properties of uncoated and coated Ti2 and Ti5 disks, have been investigated in terms of defect dimensions and roughness description. After characterizing Ti2 and Ti5 substrates, osteoblast adhesion assays have been carried out to correlate roughness parameters and the amount of cell adhesion. The results obtained suggest that sodium alginate hydrogel is the most capable material among those which have been tested, since it allows to preserve adequate roughness properties. By means of correspondence analysis it has been also possible to identify one roughness parameters (peak density) which has been demonstrated to be the main factor in controlling osteoblast adhesion. These findings might help in addressing the design of innovative coating devices able to deliver biochemical signals and promote, at the same time, bone cell adhesion. Further investigations will be aimed at measuring the kinetic of release of already synthesized adhesion peptides from sodium alginate hydrogel; afterwards, the peptide-enriched coating will be applied on real implants and its capacity of promoting the osseointegration process will be evaluated in vivo.

Acknowledgements

Authors would like to acknowledge Dr. Franco Bonollo (Department of Management and Engineering, University of Padova) for optical microscope and SEM images; Dr. Stefania Turato (Italian National Council of Research, Padova) for contact profilometry analysis. This work has been in part supported by grant of the University of Padova (Progetto di Ricerca di Ateneo n CPDA017573).

References

[1] MacDonald DE, Markovic B, Boskey AL, Somasundaran P. Physico-chemical properties of human plasma fibronectin binding to well characterized titanium dioxide. Colloids Surf 1998;11: 131–9.

[2] Ramires PA, Giuffrida A, Milella E. Three-dimensional reconstruction of confocal laser microscopy images to study the behavior of osteoblastic cells grown on biomaterials. Biomaterials 2002;4:397–406.

[3] Kasemo B, Gold J. Implant surfaces and interface processes. Adv Dent Res 1999;13:8–20.

[4] Puleo DA, Nanci A. Understanding and controlling the bone–implant interface. Biomaterials 1999;20:2311–21.

[5] Boyan BD, Hummert TW, Dean DD, Schwartz Z. Role of material surfaces in regulating bone and cartilage cell response. Biomaterials 1996;17:137–46.

[6] Healy E, Thomas CH, Rezania A, Kim JE, McKeown PJ, Lom B, Hockberger PE. Kinetics of bone cell organization and mineralization on materials with patterned surface chemistry. Biomaterials 1996;17:195–207.

[7] Nishiguchi S, Kato H, Neo M, Oka M, Kim H-M, Kokubo T, Nakamura T. Alkali- and heat treated porous titanium for orthopedic implants. J Biomed Mater Res 2001;54:198–208.

[8] Hunter A, Archer CW, Walker PS, Blunn GW. Attachment and proliferation of osteoblasts and fibroblasts on biomaterials for orthopedic use. Biomaterials 1995;16:287–95.

[9] Larsson C, Thomsen P, Aronsson B-O, Rodhal M, Lausmaa J, Kasemo B, Ericson LE. Bone response to surface-modified titanium implants: studies on the early tissue response to machined and electropolished implants with different thickness. Biomaterials 1996;17:605–16.

[10] Cochran DL, Schenk RK, Lussi A, Higginbottom F, Buser D. Bone response to unloaded and loaded titanium implants with sandblasted and acid-etched surface: a histometric study in the canine mandible. J Biomed Mater Res 1998;40:1–11.

[11] Bigerelle M, Anselme K, Noël B, Ruderman I, Hardouin P, Iost A. Improvement in the morphology of Ti-based surfaces: a new process to increase in vitro human osteoblast response. Biomaterials 2002;23:1563–77.

[12] Anselme K, Linez P, Bigerelle M, Le Maguer D, Le Maguer A, Hardouin P, Hildebrand HF, Iost A, Leroy JM. The relative influence of the topography and chemistry of TiAl6V4 surfaces on osteoblastic cell behavior. Biomaterials 2000;21: 1567–77.

[13] Saterbak A, Lauffenburger DA. Adhesion mediated by bonds in series. Biotechnol Prog 1996;12:682–99.

[14] Dee KC, Rueger DC, Andersen TT, Bizios R. Conditions which promote mineralization at the bone–implant interface: a model in vitro study. Biomaterials 1996;17:209–15.

[15] Dee KC, Andersen TT, Bizios R. Design and function of novel osteoblast-adhesive peptides for chemical modification of biomaterials. J Biomed Mater Res 1998;40:371–7.

[16] Ferris DM, Moodie GD, Dimond PM, Gioranni CWD, Ehrlich MG, Valentini RF. RGD-coated titanium implants stimulate increased bone formation in vivo. Biomaterials 1999;20: 2323–31.

[17] Heid S, Effenberger F, Bierbaum K, Grunze M. Self-assembled mono- and multilayers of terminally functionalised organosilyl compounds on silicon substrates. Langmuir 1996;12: 2118–20.

[18] Tidwell CD, Ertel SI, Ratner BD, Tarasevich BJ, Atre S, Allara DL. Endothelial cell growth and protein adsorption on terminally functionalized, self-assembled monolayers of alkanethiolates on gold. Langmuir 1997;13:3404–13.

[19] Healy KE, Rezania A, Stile RA. Designing biomaterials to direct biological response. Ann New York Acad Sci 1999;875: 24–35.

[20] Glass JR, Dickerson KT, Stecker K, Polarek JW. Characterization of a hyaluronic acid-Arg-Gly-Asp peptide cell attachment matrix. Biomaterials 1996;17:1101–8.

[21] Heckman JD, Ehler W, Brookes BP, Aufdemorte TB, Lohmann CH, Morgan T, Boyan BD. Bone morphogenetic protein but not transforming growth factor-β enhances bone formation in canine diaphyseal nonunions implanted with a biodegradable composite polymer. J Bone Jt Surg 1999;81:1717–29.

[22] Suzuki Y, Tanihara M, Suzuki K, Saitou A, Sufan W, Nishimura Y. Alginate hydrogel linked with synthetic oligopeptide derived from BMP-2 allows ectopic osteoinduction in vivo. J Biomed Mater Res 2000;50:405–9.

[23] Rickard DJ, Sullivan TA, Shenker BJ, LeBoy PS, Kazhdan I. Induction of rapid osteoblast differentiation in rat bone marrow stromal cell cultures by dexamethasone and BMP-2. Dev Biol 1994;161:218–28.
[24] Yokose S, Ishizuya T, Ikeda T, Nakamura T, Tsurukami H, Kawasaki K, Suda T, Yoshiki S, Yamaguchi A. An estrogen deficiency caused by ovariectomy increases plasma levels of systemic factors that stimulate proliferation and differentiation of osteoblasts in rats. Endocrinology 1996;137: 469–78.
[25] Luna LG. Manual of histologic staining methods of the armed forces institute of pathology. In: Luna LG, editor. New York: McGraw-Hill; 1968. p. 174–88.
[26] Benzecry J. Correspondence analysis handbook. New York: Marcel Dekker; 1992.
[27] Dekker P. L'analyse factorielle. Paris: PUF; 1994.
[28] Greenacre MJ. Correspondence analysis in practice. London: Academic Press; 1993.
[29] Gower JC. Biplots. Chapman & Hall/CRC: London/Boca Raton, FL; 1995.